PHILOSOPHICAL TRANSACTIONS OF THE ROYAL SOCIETY A MATHEMATICAL, PHYSICAL & ENGINEERING SCIENCES

Analytical Determination of Bifurcations in an Impact Oscillator

Stephen Foale

Phil. Trans. R. Soc. Lond. A 1994 **347**, 353-364
doi: 10.1098/rsta.1994.0048

Analytical determination of bifurcations in an impact oscillator

By Stephen Foale

Centre for Nonlinear Dynamics, University College London, Gower Street, London WC1E 6BT, U.K.

It is well known that some solutions for a sinusoidally driven oscillator with linear stiffness and impacts at rigid stops modelled with a coefficient of restitution impact law can be located analytically. Recently, new co-dimension one bifurcations called grazing bifurcations have been found in such systems. Here we present analytical results which show how the type of grazing bifurcation changes with parameter, and that when the type of grazing bifurcation changes a codimension two bifurcation occurs. The simplest grazing bifurcations involve orbits of period-1, but we show that the same analytical methods can be used to locate some subharmonics and their bifurcations.

1. Introduction

Many studies have highlighted the practical physical and engineering problems which involve rigid impacts between two components. Mechanical engineering provides many examples of systems with impacts such as rattling gears (Karagiannis & Pfeiffer 1991; Kahraman & Singh 1990), vibration absorbers (Sharif-Bakhtiar & Shaw 1988), car suspensions (Stennson *et al.* 1992) and impact print hammers (Tung & Shaw 1988). In these mechanical engineering examples of impact oscillators, the primary problems caused by the successive impacts are noise and wear. Another rich source of impact oscillator problems is the offshore engineering environment. Work by Thompson and co-workers on the problem of a ship moored to an articulated mooring tower, essentially an inverted pendulum with buoyancy, undergoing wave driven oscillations was extensively studied (Thompson 1983; Thompson *et al.* 1984). A similar problem, that of a ship moored against a fender, was studied by Lean (1971) and more recently, by Sterndorff *et al.* (1992). Other offshore impacting problems arise in the installation of a structure over a guiding 'indexing' system, discussed in more detail in Foale (1993). Indexing systems can be comprised of bumper piles, which guide the structure into position (Nelson *et al.* 1983; Stahl *et al.* 1983) or pile/sleeve arrangements (Robinson & Ramzan 1989). The effect of earthquakes on various structures has motivated other studies of dynamical impact type problems, for example, the responses of a slender block which rocks under external excitation (Hogan 1989; Tso & Wong 1989). The 'pounding' (i.e. collision) of nearby buildings under earthquake excitation is another example (Jing & Young 1990). The electricity generating industry has also produced impact oscillator problems, such as the cross flow induced impacting of heat exchanger tubes (Paidoussis & Li 1992).

It was noted in Shaw & Holmes (1983) that low velocity impacts in these simple one impact steady-state solutions lead to discontinuities in the gradient of the *impact*

Proc. R. Soc. Lond. A (1994) **347**, 353–364
Printed in Great Britain

map (see §4). This observation has been expanded on in work by Nordmark (1991), Foale & Bishop (1992) and Budd *et al.* (1993) amongst others. A new kind of bifurcation, the *grazing bifurcation*, has been found to occur whenever part of an orbit just touches (or grazes) a stop. In this paper we use the analytical solutions to investigate further the types of grazing bifurcation which can occur and find both codimension one and codimension two bifurcations.

2. The impact oscillator model

There are several different ways in which the impact can be modelled in an impact oscillator. Probably the simplest is the coefficient of restitution rule, $\dot{x} \to -r\dot{x}$, which is applied when a stop is reached. This rule provides an instantaneous reversal of velocity and, if the coefficient of restitution $r < 1$, a loss of energy at the impact. Other approaches to modelling the impact have been to use a stiffness function which rapidly increases after impact, such as a piecewise linear stiffness (Shaw & Holmes 1983) or the Hertz impact law (Jing & Young 1990; Foale & Bishop 1994*a*). Away from the stop, we assume that the equation governing the motion is the simple forced linear oscillator given by

$$\ddot{x} + d\dot{x} + x = \alpha \cos(\omega t), \quad x < a, \tag{1}$$

which is valid when the displacement $x < a$, where $x = a$ is the position of the stop. In (1) an overdot represents differentiation with respect to the time t, d is the linear damping coefficient, α the amplitude of the forcing function and ω the forcing frequency. In almost all cases, one more system parameter can be eliminated from the above by rescaling the displacement, x, so the stop is at $x = 1$. However, this rescaling rules out the special case of $x = 0$, so we will use the above form. In (1) we assume that time and displacement have been rescaled in order to scale to one any mass or stiffness terms. We also note that variation of the forcing amplitude α is directly equivalent (after rescaling) to adjusting the position of the stop. A further rescaling of x by putting $x \to \alpha x$ in (1) gives exactly the same linear oscillator with the stop at a/α, i.e. increasing the amplitude of the forcing by some factor is equivalent to moving the stop closer to the equilibrium position by the same factor. In addition to (1), when the displacement x reaches the position of the stop $x = a$ the rule

$$\dot{x} \to -r\dot{x}, \quad x = a \tag{2}$$

is applied, where the coefficient of restitution r lies in the range $0 < r \leqslant 1$. This coefficient r is determined empirically for the impact between two surfaces. After (2) has been applied, the linear oscillator (1), takes over again.

3. Locating steady-state periodic solutions

Away from any impacts the coefficient of restitution (COR) impact oscillator (1) is just a sinusoidally forced linear ordinary differential equation which we can easily solve exactly. We can write the solution for the displacement x at time t in the form

$$x = \mathrm{e}^{-\beta(t-t_\mathrm{i})} F(x_\mathrm{i}, y_\mathrm{i}, t_\mathrm{i}; t) - (\alpha/\gamma)\cos(\omega t + \phi), \tag{3}$$

where x_i, y_i are the initial displacement and velocity respectively at time t_i. Differentiating this with respect to t gives

$$\dot{x} = \mathrm{e}^{-\beta(t-t_\mathrm{i})} G(x_\mathrm{i}, y_\mathrm{i}, t_\mathrm{i}; t) + (\alpha\omega/\gamma)\sin(\omega t + \phi), \tag{4}$$

where F and G are known functions of the parameters, initial conditions and time and

$$\tan\phi = d\omega/(\omega^2-1), \quad \gamma = \sqrt{[(d\omega)^2+(\omega^2-1)^2]}, \quad 2\beta = d. \tag{5}$$

The simplest steady-state solutions with impacts of the system defined by (1) are of period-1 (i.e. they repeat once in a complete forcing cycle) and undergo only one impact per period. In order to locate such solutions we impose these conditions on the general solution for (1) given above. We take initial conditions at the stop $(x, \dot{x}, t) = (a, y_i, t_i)$ before imposing the COR rule. After applying the impact rule we have $(x, \dot{x}, t) = (a, -ry_i, t_i)$ which defines the constants of integration in terms of the unknowns y_i and t_i. Then (3) and (4) are equations for x and $\dot{x}$ as functions of y_i, t_i and time t. By adding the matching conditions which need to be satisfied at a steady state period-1, one impact per period, periodic orbit we have the conditions that $x(t_i+2\pi/\omega; y_i, t_i) = a$, $\dot{x}(t_i+2\pi/\omega; y_i, t_i) = y_i$. Using these conditions, (3) and (4) can be rewritten by collecting together terms in $c_i = \cos(\omega t_i+\phi)$, $s_i = \sin(\omega t_i+\phi)$, and constants depending only on the parameters to give

$$-ry_i = l_1 c_i + l_2 s_i + l_3, \tag{6}$$

$$0 = m_1 c_i + m_2 s_i + m_3, \tag{7}$$

where

$$l_1 = (\Omega\mu/s_w)[(1/v)-c_w]-\mu\beta, \quad l_2 = \mu\omega, \quad l_3 = (a/\mu)\, l_1, \tag{8}$$

$$m_1 = \frac{l_1}{r}+v\mu\left\{\frac{\Omega c_w}{s_w}\left(\frac{1}{v}-c_w\right)-\Omega s_w-\frac{\beta}{v}\right\}, \quad m_2 = \mu\omega\left(1+\frac{1}{r}\right), \quad m_3 = \frac{a}{\mu}m_1, \tag{9}$$

$$\left.\begin{aligned} \mu = \alpha/\gamma, \quad v = \mathrm{e}^{-\beta(t_f-t_i)}, \quad c_w = \cos[\Omega(t_f-t_i)], \\ s_w = \sin[\Omega(t_f-t_i)], \quad t_f-t_i = 2\pi/\omega, \quad \Omega = \sqrt{(1-\beta^2)}. \end{aligned}\right\} \tag{10}$$

Now if we treat (6) and (7) as simultaneous equations in c_i and s_i we can obtain

$$s_i = \frac{ry_i}{(m_2/m_1)(l_1-l_2)}, \quad c_i = -\frac{(m_2/m_1)ry_i}{(m_2/m_1)(l_1-l_2)}-\frac{m_3}{m_1}, \tag{11}$$

and we can eliminate time completely by noting that $c_i^2+s_i^2 = 1$, i.e.

$$\frac{r^2y_i^2}{((m_2/m_1)(l_1-l_2))^2}[1+(m_2/m_1)^2]+2(m_3/m_1)\frac{(m_2/m_1)ry_i}{(m_2/m_1)(l_1-l_2)}+(m_3/m_1)^2 = 1. \tag{12}$$

This is a quadratic equation in y_i which we can easily solve. Then by substituting y_i into (11) we have an expression for the other unknown quantity t_i. Therefore, at a given set of parameters we have possible solutions for y_i and t_i that define a point on a steady-state, period-1, one impact per period orbit of the system defined by equations (1) and (2). It is only a possible solution: we must ensure that $x = a$ at times t_i and $t_i+(2\pi/\omega)$ but at no time in between, since this would correspond to a non-physical orbit.

4. Stability analysis of period-1, one impact solutions

We have given above a method for locating a point on a steady-state, period-1, one impact per period orbit of the impact oscillator defined in §2. Since this point is always on the plane $x = a$ (the stop) we can regard it as a fixed point of the mapping which takes this plane onto itself. This *impact map* is one of the 'natural' Poincaré maps which can be defined by taking a section almost everywhere transverse to the

flow. It is only almost everywhere transverse to the flow since along the zero velocity line $\dot{x} = 0$ the flow is always tangential to the plane $x = a$. If we differentiate (3) and (4) with respect to the initial time and velocity t_i and y_i and evaluate at $t_f = t_i + (2\pi/\omega)$, we can obtain the elements of the first differential matrix of the mapping from the stop at negative velocity to the corresponding point at the stop with positive velocity, one period later. There is an extra simple contribution to the final jacobian matrix $\boldsymbol{D}$ from the coefficient of restitution rule. Determining the jacobian of the fixed point of the impact in this way, we can obtain expressions for the trace and determinant of $\boldsymbol{D}$, $\mathrm{tr}\,(\boldsymbol{D})$ and $\det(\boldsymbol{D})$ respectively:

$$\det(\boldsymbol{D}) = v^2 r^2,$$
$$\mathrm{tr}\,(\boldsymbol{D}) = 1 - rvc_w - (\beta v r s_w/\Omega) + (s_i\,\mu\omega/y_i)\,[(\beta v s_w/\Omega)(1+2r) + vc_w - 1] + (vc_i\,s_w/\Omega y_i)\,[\mu\omega^2 - \mu r + \mu\omega^2 r - ar]. \quad (13)$$

The eigenvalues of the mapping are given by

$$\lambda_{1,2} = \tfrac{1}{2}[\mathrm{tr}\,(\boldsymbol{D}) \pm \sqrt{[\mathrm{tr}\,(\boldsymbol{D})^2 - 4\det(\boldsymbol{D})]}] \quad (14)$$

and so it is clear that as $y_i \to 0$ one of the eigenvalues will tend to either positive or negative infinity (and since the map is dissipative overall and the product of the eigenvalues equals the determinant, the other eigenvalue must tend to zero with the same sign). Steady-state solutions with very low velocity impacts will therefore be saddle solutions with one direction of large expansion and one of large contraction. A grazing bifurcation occurs at parameter values where the velocity of the impact of steady-state periodic orbit equals zero.

5. Bifurcations of period-1, one impact solutions

The impact oscillator defined in §2, as well as undergoing conventional, smooth bifurcations (flips and saddle-nodes), can undergo bifurcations due to low velocity impacts, called grazing bifurcations (see, for example, Nordmark 1991; Foale & Bishop 1992). It can be shown that there are discontinuities in gradient in any Poincaré map from an impact oscillator along lines of grazing points (see, for example, Foale & Bishop 1994*b*). If a fixed point crosses a line of grazing points under the change of a system parameter then a grazing bifurcation occurs. In this section we look at the simplest case of a grazing bifurcation in the one sided, linear impact oscillator, (1) and (2), where a non-impacting period-1 stable steady-state solution, under a change in parameter, just starts to hit the stop with low velocity.

Non-impacting steady-state solutions of the impact oscillator defined in §2, where they exist, just consist of the 'particular integral' part of the general solution, (3), after the transients have exponentially decayed away. We form a discrete time dynamical system from the continuous time one, in the usual way, by taking a surface of section Σ and defining the Poincaré map $\boldsymbol{P}$ which takes a point in Σ back onto itself. In this case it is most convenient to use the stroboscopic Poincaré section where x and $\dot{x}$ are sampled at a given phase of the forcing function, $\phi = t \bmod (2\pi/\omega) = 0$. From (3) and (4), fixed points of this map corresponding to non-impacting periodic steady-state solutions are easily seen to be given by $x_n = -\alpha\cos(\phi)/\gamma$, $\dot{x}_n = \alpha\omega\sin(\phi)/\gamma$, and the first differential matrix of this mapping is obtained by differentiating these equations with respect to x_i and $\dot{x}_i$ and evaluating at time $t = 2\pi/\omega$. The eigenvalues of this mapping can then be calculated to

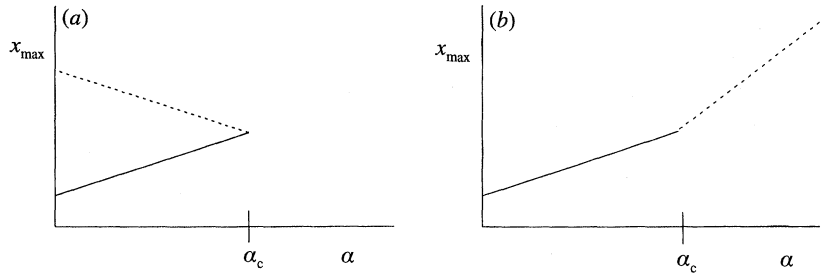

Figure 1. Two types of first grazing bifurcation. (*a*) $z < 0$; (*b*) $z > 0$.

be $\lambda_{1,2} = v(-c_w \pm s_w)$. We can see that the maximum displacement x of the non-impacting solution is α/γ, so when $\alpha/\gamma < a$ the steady-state, non-impacting orbit does exist. At a critical, grazing value of α, $\alpha_c = a\gamma$, the non-impacting orbit will just graze the stop at $x = a$ with zero velocity. As α is increased past α_c this stable orbit, or the stable fixed point of the stroboscopic map, can no longer exist. It disappears at a grazing bifurcation. The locus of these grazing bifurcations is given by

$$\alpha_c = a\gamma = a\sqrt{[(d\omega)^2 + (\omega^2 - 1)^2]}. \tag{15}$$

6. Types of first grazing bifurcation

We have discussed above how the simple, non-impacting stable solution reaches a critical point at which the amplitude of the solution is such that part of the orbit is just grazing the stop with zero velocity. In order to form a continuous solution path, a period-1 solution with one low amplitude impact per period must continue on from the end of this stable path. To see that this is so we look again at the analytical solutions for period-1, one impact per period solutions of the impact oscillator defined by (1) and (2).

We take (12), the quadratic equation in y_i, and by further noting that the parameter α only occurs in l_1, l_2, l_3, m_1, m_2, m_3 linearly (if at all) we can define new quantities L_1, L_2, L_3, M_1, M_2, M_3 all independent of α.

$$l_1 = \alpha L_1, \quad l_2 = \alpha L_2, \quad l_3 = L_3, \quad m_1 = \alpha M_1, \quad m_2 = \alpha M_2, \quad m_3 = M_3. \tag{16}$$

Then (12) can be rearranged to give

$$\alpha^2 = \alpha_c^2 + 2\alpha_c r y_i \frac{M_2/M_1}{(M_2/M_1)(L_1 - L_2)} + r^2 \frac{y_i^2}{[(M_2/M_1)(L_1 - L_2)]^2}[1 + (M_2/M_1)^2]. \tag{17}$$

From (17) we can see that near grazing, when $0 < y_i \ll 1$ then $\alpha \to \alpha_c$ from above or below depending on the sign of the coefficient of the linear term of this quadratic in y_i. As $r, y_i, \alpha_c > 0$ we have that the sign of z, where

$$z = \frac{\gamma v(1 + 1/r)\sin(2\pi\Omega/\omega)}{\Omega[1 + v^2 - 2v\cos(2\pi\Omega/\omega)]}, \tag{18}$$

controls the type of grazing bifurcation. There are two distinct types of grazing bifurcation depending on whether z is positive or negative: the two cases are sketched in figure 1, where the maximum amplitude of the period-1 solutions are plotted against the forcing amplitude α with all other parameters fixed. In both cases when $\alpha < \alpha_c$ there is a stable non-impacting period-1 solution whose amplitude grows

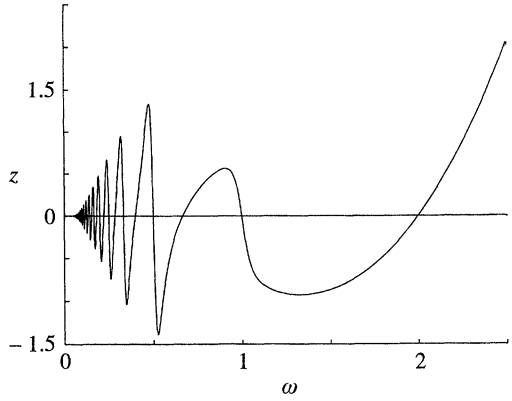

Figure 2. The function z against ω.

linearly with α (the solid lines). The stability characteristics of this non-impacting solution do not change as α changes as can be seen from the expression in §6. In figure 1*a*, with $z < 0$, as the velocity of the period-1, one impact solution $y_i \to 0$, $\alpha \to \alpha_c$ from below, with $\alpha = \alpha_c$ when $y_i = 0$. Because the velocity at impact, y_i, is very small, we can see from (13) that this solution is very unstable, with one eigenvalue tending to infinity as $\alpha \to \alpha_c$. In figure 1*b*, with $z > 0$, as the velocity of the period-1, one impact solution $y_i \to 0$, $\alpha \to \alpha_c$ from above, with $\alpha = \alpha_c$ when $y_i = 0$. Again the velocity at impact, y_i, is very small and so this solution is very unstable, with one eigenvalue tending to infinity as $\alpha \to \alpha_c$. These unstable solutions are represented by dotted lines in figure 1.

On examining the expression for z we see that $z = 0$ when $s_w = \sin(2\pi\Omega/\omega) = 0$, i.e. when $\omega = 2\Omega/n$ for $n = 1, 2, \ldots$. These are the values of ω where the function z changes sign (see figure 2).

7. Illustrations of grazing bifurcations

Using the method described in §3 we are able to locate analytically steady-state period-1 solutions of the impact oscillator defined in §2, both for the case of non-impacting and one impact per period solutions. We must always numerically ensure that the one impact per period orbits are physically possible, i.e. that the orbit is at displacement $x = a$ at the fixed point in the impact map and one period later but at no time in between. We numerically check that the possible analytical solution is valid by time stepping along the known analytical solution away from the stop, checking at each step that $x < a$. It should be stressed that numerics are only used to check that the analytically determined steady-state solution is physically possible. The stability analysis (§4) allows us to monitor the stability of the periodic orbits found in this way. Using these methods we semi-analytically, semi-numerically obtain the amplitude-response diagrams (figure 3), where the maximum absolute displacement $\max(x)$ is plotted against α. Here, all parameters are kept fixed ($d = 0.1$, $r = 0.7$, $a = 1.0$, $\omega = 1.8, 2.2$) except the amplitude of the forcing α: solid lines denote stable solutions and dotted lines unstable solutions. The two cases are taken at constant values of the forcing frequency, ω, either side of the largest value of ω at which the function z (18) changes sign, $\omega = 2\Omega \approx 1.9975$, and illustrate the two types of grazing bifurcation described in the previous section.

PHILOSOPHICAL TRANSACTIONS OF THE ROYAL SOCIETY A MATHEMATICAL, PHYSICAL & ENGINEERING SCIENCES

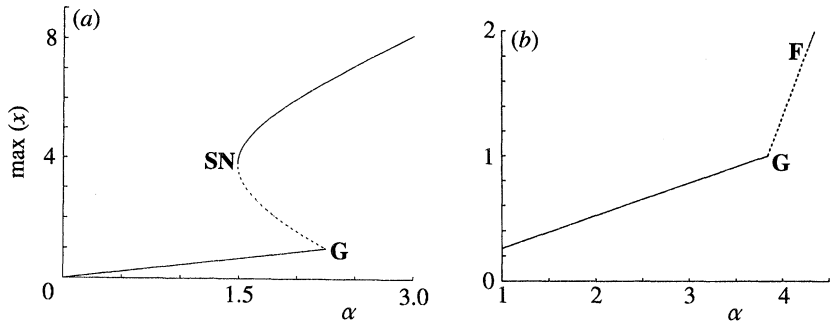

Figure 3. The path of period-1, one impact solutions of the one sided impact oscillator with (*a*) $\omega = 1.8$; (*b*) $\omega = 2.2$.

In the first case, illustrated in figure 3*a* we fix the forcing parameter $\omega = 1.8$. As α is increased from zero up to the critical, first grazing value $\alpha_c \approx 2.247$, there exists a linearly increasing path of the stable non-impacting period-1 solution. This solution must disappear at grazing. As the function z here is less than zero, it was shown in §6 that a period-1, one impact per period solution exists as α approaches the first grazing parameter value α_c from below, and as the velocity at impact tends to zero, an eigenvalue of the impacting solution tends to infinity as grazing is approached. We see than a grazing bifurcation in figure 3*a* at ***G*** where a stable and unstable solution meet and disappear together. As the path continues there is a saddle-node bifurcation at ***SN***. There are similarities between the two bifurcations, ***G*** and ***SN***, because in both cases stable and unstable solutions meet and annihilate one another. However, the two are quite different. At ***SN*** the stability characteristics of the two orbits change smoothly, with an eigenvalue tending to $+1$ from above and below. At ***G***, the stability characteristics of the stable solution do not change up to grazing, but an eigenvalue of the unstable solution tends to infinity as grazing is approached.

The second illustration of a grazing bifurcation is shown in figure 3*b* where $\omega = 2.2$. Again, as α is increased up to the critical, first grazing value $\alpha_c \approx 3.846$, there exists a linearly increasing path of the stable non-impacting period-1 solution. The function z here is greater than zero, so the period-1, one impact per period solution approaches the first grazing parameter value α_c from above. Again, since the velocity at impact tends to zero as $\alpha \to \alpha_c$ from above, an eigenvalue of the impacting period-1 solution tends to infinity as the grazing bifurcation ***G*** is approached. In this case, as the path continues, there is a flip bifurcation at ***F***.

8. Bifurcation loci of smooth and grazing bifurcations

In §5, equation (15) was derived, which gives the locus of first grazing bifurcations in terms of the system parameters. If, as in §7, we fix all of the parameters except α and ω, then as the forcing frequency ω varies the first grazing (the solid curve in figure 4) occurs at α_c. Using the analytical expression for the eigenvalues of the period-1, one impact solution (14), we can compute numerically the loci of flip bifurcations where an eigenvalue equals -1, and saddle-node bifurcations where an eigenvalue equals $+1$. Figure 4 shows the locus of flip bifurcations as a dotted line and the locus of saddle-node bifurcations as a chain dotted line. Below $\omega = 0.5$ there are further alternating flip and saddle node bifurcations, but the loci of these bifurcations have not been computed here. It appears that the flip and saddle-node

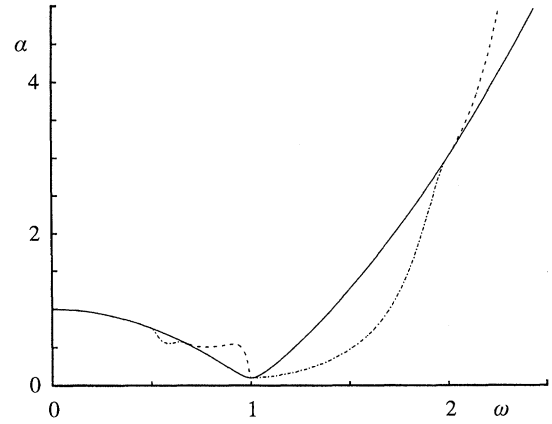

Figure 4. Bifurcation loci of period-1 solutions for the one sided impact oscillator.

loci meet at the values of ω where the function z passes through zero (equation 18, figure 2) and the type of grazing bifurcation changes. In the next section we show that this is indeed the case.

9. Co-dimension two bifurcations

As noted in the previous section, it appears in the bifurcation locus diagram figure 4 that when the type of grazing bifurcation changes, i.e. when the sign of z changes, then a line of saddle-node bifurcations and a line of flip bifurcations meet at this point. We now demonstrate that this is indeed the case. Let $2\pi\Omega/\omega = \pi + \epsilon$. Then $s_w = -\sin(\epsilon)$, $c_w = -\cos(\epsilon)$. If we substitute these expressions into (13), using (11) for s_i and c_i, we have an expression for $\mathrm{tr}(\boldsymbol{D})$ in ϵ. Expanding this in powers of the small variable ϵ we have

$$\mathrm{tr}(\boldsymbol{D}) = 2vr + \frac{av\omega^2(1+r)}{\Omega}\frac{\epsilon}{y_i} + \frac{2\beta v(1+r)(vr-1)}{\Omega(v+1)}\epsilon + O(\epsilon^2). \tag{19}$$

The small variable ϵ depends on the driving frequency ω, not on the amplitude of the forcing α, and so however small ϵ is, we can choose α close enough to α_c such that y_i is as small as we like, and so ϵ/y_i is of $O(1)$ or greater. Any term in ϵ can therefore be ignored as small.

The condition which must be satisfied for a saddle-node bifurcation is

$$\det(\boldsymbol{D}) - \mathrm{tr}(\boldsymbol{D}) + 1 = 0 \tag{20}$$

and for a flip bifurcation,

$$\det(\boldsymbol{D}) + \mathrm{tr}(\boldsymbol{D}) + 1 = 0, \tag{21}$$

so we define $sn = \det(\boldsymbol{D}) - \mathrm{tr}(\boldsymbol{D}) + 1$ and $pd = \det(\boldsymbol{D}) + \mathrm{tr}(\boldsymbol{D}) + 1$. Using (19) for $\mathrm{tr}(\boldsymbol{D})$ gives, to leading order

$$sn = (rv-1)^2 - K\epsilon/y_i + \ldots, \tag{22}$$

$$pd = (rv+1)^2 + K\epsilon/y_i + \ldots, \tag{23}$$

where $K = av\omega^2(1+r)/\Omega > 0$. The condition for a saddle-node bifurcation, $sn = 0$, then gives

$$sn = 0 \Rightarrow y_i = K\epsilon/(rv-1)^2 + \ldots. \tag{24}$$

The velocity at impact of the steady-state, period-1, one impact solution, y_i, must be positive, and this can only be so if $\epsilon > 0$ in (24) above. Thus we conclude that when ϵ is small and positive (i.e. $\omega < 2\Omega$) there is a period-1, one impact steady-state solution which is undergoing a saddle-node bifurcation. For a given small positive ϵ the parameter α_{sn} at which this bifurcation occurs can be obtained from (17). Since $\omega < 2\Omega$ the function z which controls the type of grazing bifurcation nearby is negative, so $\alpha_{sn} < \alpha_c$ and $\alpha_{sn} \to \alpha_c$ as $\epsilon \to 0$, i.e. as $\omega \to 2\Omega$ from below. The amplitude of forcing, α, at which the saddle-node bifurcation occurs can be seen from (17) to be

$$\alpha_{sn} = \sqrt{\left[\alpha_c^2 + \frac{2\alpha_c rzK}{(rv-1)^2}\epsilon + \ldots\right]}. \tag{25}$$

Similarly, the condition for a flip bifurcation, $pd = 0$, gives

$$pd = 0 \Rightarrow y_i = -K\epsilon/(rv+1)^2 + \ldots. \tag{26}$$

Again, we must have that y_i is positive, and this can only be so if $\epsilon < 0$ in (26). Thus we conclude that when ϵ is small and negative (i.e. $\omega > 2\Omega$) there is a period-1, one impact steady-state solution which is undergoing a flip bifurcation. For a given small negative ϵ the parameter, α_{pd}, at which this bifurcation occurs can be obtained from (17). As $\omega > 2\Omega$ the variable z which controls the type of grazing bifurcation nearby is positive, so $\alpha_{pd} > \alpha_c$ and $\alpha_{pd} \to \alpha_c$ as $\epsilon \to 0$, i.e. as $\omega \to 2\Omega$ from above. The amplitude of forcing α at which the flip bifurcation occurs can be seen from (17) to be

$$\alpha_{pd} = \sqrt{\left[\alpha_c^2 + \frac{2\alpha_c rzK}{(rv+1)^2}\epsilon + \ldots\right]}. \tag{27}$$

In summary then, the above analysis has shown that at a point where the sign of z changes, and therefore the type of grazing bifurcation changes, there are additional lines of saddle-node bifurcations and flip bifurcations which meet at the same point in the space spanned by the two parameters α and ω. This is a codimension 2 bifurcation point because two parameters are needed to contain the bifurcation in a persistent way. Similar results to those in this section are contained in Ivanov (1993).

10. Bifurcations of subharmonics

In §3 we derived expressions for possible solutions to the impact oscillator defined by equations (1) and (2) with period-1 and one impact per period. Almost exactly the same analysis can be used to locate subharmonics of the same model with one impact in N forcing periods where $N = 2, 3, 4, \ldots$. The only changes which are required are that instead of looking for an orbit which repeats after time T (one period) we look for one which repeats after time NT (N periods). In equation (10) then we just put $t_f - t_i = 2\pi N/\omega$, which modifies the constants v, c_w and s_w. The procedure for locating possible steady-state solutions is then identical to that for period-1 solutions. First, the quadratic equation (12) is solved for the velocity at impact y_i and this is then substituted into equation (11) to solve for the time at impact, t_i. The possible solution given by this procedure must be verified numerically to ensure it is a true, physical solution. The jacobian matrix of the impact map for period-N solutions is obtained by substituting the modified constants v, c_w and s_w into equation (13). Then equation (14) gives the eigenvalues of the jacobian of the impact mapping exactly as before.

Using the expressions for the eigenvalues of the jacobian we can locate the loci of saddle-node and flip bifurcations of period-N, one impact steady-state solutions as in

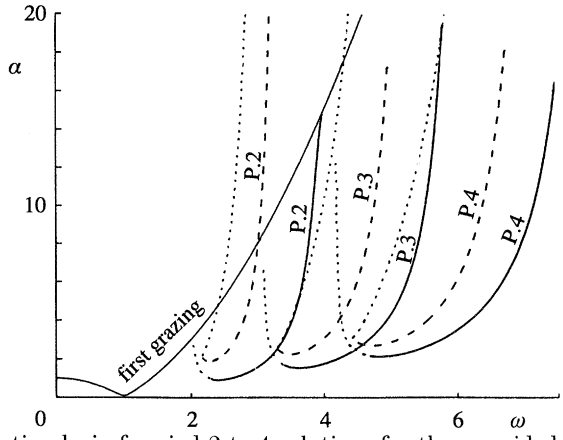

Figure 5. Bifurcation loci of period-2 to 4 solutions for the one sided impact oscillator. Saddle node ——; flip – – –; grazing · · · · ·.

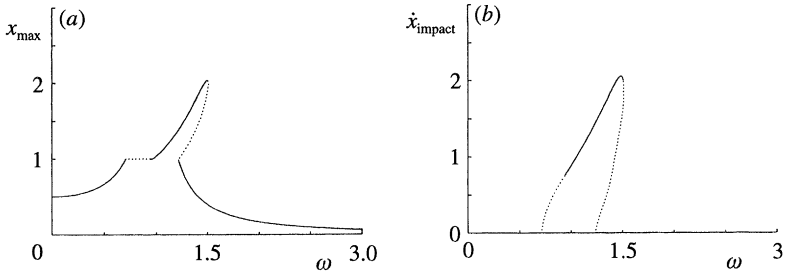

Figure 6. Frequency response diagram showing one impact period-1 solutions for the one sided impact oscillator; $\alpha = 0.5$.

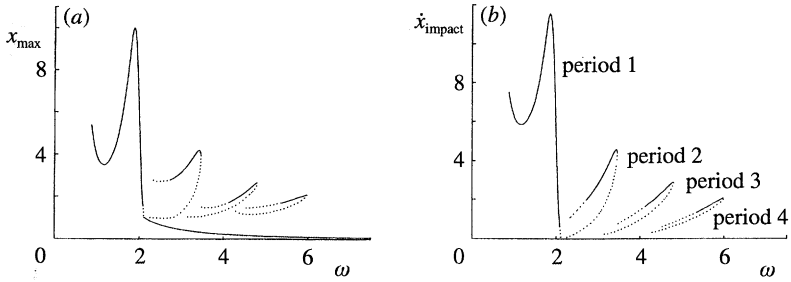

Figure 7. Frequency response diagram showing one impact period-1 to 4 solutions for the one sided impact oscillator; $\alpha = 3.5$.

§4. The loci of these bifurcations for steady-state, one impact solutions of periods-2, 3 and 4 are shown in figure 5 as the two parameters α and ω are varied. Also shown in this figure are the lines of grazing bifurcations. Again all other parameters are fixed as in §7.

Frequency response curves for two fixed forcing amplitudes are shown in figures 6 and 7, where all other parameters are fixed as in §7. Both the maximum absolute displacement, x_{max} and the maximum velocity at impact $\dot{x}_{max}$ over N forcing cycles are shown plotted against the forcing frequency ω. Stable solutions are represented by a solid line whilst unstable solutions are shown with a dotted line. Only the period-N, one impact steady-state solutions are shown in these figures, i.e. those which can

be calculated analytically. In figure 6 the forcing parameter is kept fixed at $\alpha = 0.5$. In this case there are two 'first grazing' bifurcations either side of the linear natural frequency $\omega = 1$. As the forcing frequency is increased from zero there is a stable non-impacting limit cycle whose amplitude grows as the frequency is increased towards 1. First grazing bifurcations occur at $\omega \approx 0.710$ and $\omega \approx 1.218$, of 'flip type' and 'saddle-node type' respectively. The overall shape of this frequency response curve is typical for small forcing amplitudes. All of the solutions shown in figure 6 are of period-1, and no higher period, one impact solutions were found at this low forcing amplitude. Figure 7 shows the response curves up to period 4 for $\alpha = 3.5$. In this figure there is only one first grazing bifurcation, at $\omega \approx 2.119$. The higher period, one impact solutions all disappear as frequency ω is increased at a saddle-node bifurcation, but some appear at saddle-node bifurcations and others are created at grazing bifurcations.

11. Discussion

The observation that particular steady-state solutions of the simple COR law impact oscillator with linear stiffness and damping can be found analytically has been widely used. In this paper we have shown that using these analytical solutions much of the bifurcation structure of the COR impact oscillator, at least for simple periodic orbits, can be determined. We have used the analytical solutions to investigate not only the conventional codimension one bifurcations (flips and saddle-nodes), but also the different types of grazing bifurcation which the simple one impact per period steady-state solutions can undergo. In §9 we showed that, at the point where the type of grazing bifurcation changes, a line of flip bifurcations and a line of saddle-node bifurcations also meet at a codimension two bifurcation. In this way, we can see that the type of first grazing bifurcation, where the non-impacting stable steady-state solution just touches the stop, has a strong organizing effect on other bifurcations of period-1, one impact solutions. Finally, we have shown in §10 that higher subharmonic periodic orbits with only one impact can also be found in exactly the same way, along with the bifurcations which they undergo.

I thank the SERC Marine Technology Directorate for the support of this work.

References

Budd, C., Dux, F. & Cliffe, A. 1993 The effect of frequency and clearance on single degree of freedom impact oscillators. Internal Report AM-93-02, Bristol University.

Foale, S. 1993 Bifurcations in impact oscillators: theoretical and experimental studies. Ph.D. thesis, University of London.

Foale, S. & Bishop, S. R. 1992 Dynamical complexities of forced impacting systems. *Phil. Trans. R. Soc. Lond.* A **338**, 547–556.

Foale, S. & Bishop, S. R. 1994*a* Bifurcations in impact oscillators. *Nonlinear dynamics*. (In the press.)

Foale, S. & Bishop, S. R. 1994*b* Bifurcations in impact oscillators: theory and experiments. In *Proc. IUTAM Symp. Nonlinear Dynamics Chaos engng Dynamics*. Wiley.

Hogan, S. J. 1989 On the dynamics of rigid-block motion under harmonic forcing. *Proc. R. Soc. Lond.* A **425**, 441–476.

Ivanov, A. P. 1993 Stabilization of an impact oscillator near grazing incidence owing to resonance. *J. Sound Vib.* **162**, 562–565.

Jing, H. S. & Young, M. 1990 Random response of a single degree of freedom vibro impact system with clearance. *Earthquake engng Structural Dynamics* **19**, 789–798.

PHILOSOPHICAL TRANSACTIONS OF THE ROYAL SOCIETY A MATHEMATICAL, PHYSICAL & ENGINEERING SCIENCES

Kahraman, A. & Singh, R. 1990 Nonlinear dynamics of a spur gear pair. *J. Sound Vib.* **142**, 49–75.

Karagiannis, K. & Pfeiffer, F. 1991 Theoretical and experimental investigations of gear rattling. In *Nonlinear dynamics*, vol. 2, pp. 367–387.

Lean, G. H. 1971 Subharmonic motions of moored ships subjected to wave action. *Trans. R. Inst. nav. Architects* **113**, 387–399.

Nelson, W. E., Benton, S. M. & Bernhard, S. 1983 Bumper pile design for mating platform and subsea drilling template. Presented at *Offshore Technology Conference*, Houston.

Nordmark, A. B. 1991 Non-periodic motion caused by grazing incidence in an impact oscillator. *J. Sound Vib.* **145**, 279–297.

Nusse, H. E. & Yorke, J. A. 1992 Border collision bifurcations including 'period two to period three' for piecewise smooth systems. *Physica* D **57**, 39–57.

Paidousis, M. P. & Li, G. X. 1992 Cross-flow-induced chaotic vibrations of heat exchanger tubes impacting on loose supports. *J. Sound Vib.* **152**, 305–326.

Robinson, R. W. & Ramzan, F. A. 1989 Prediction of jacket to template docking forces during installation. Preprint.

Sharif-Bakhtiar, M. & Shaw, S. W. 1988 The dynamic response of a centrifugal pendulum vibration absorber with motion limiting stops. *J. Sound Vib.* **126**, 221–235.

Shaw, S. W. & Holmes, P. J. 1983 A periodically forced piecewise linear oscillator. *J. Sound Vib.* **90**, 122–155.

Stahl, B., Nelson, W. E. & Baur, M. P. 1983 Motion monitoring of a moored floating platform during installation over a subsea template. *J. Petroleum Tech.*, 1239–1248.

Stennson, A., Asplund, C. & Karlsson, L. 1992 The nonlinear behaviour of a MacPherson strut wheel suspension. Preprint. Lulea University of Technology, Sweden.

Sterndorff, M. J., Waegter, J. & Eilersen, C. 1992 Design of fixed offshore platforms to dynamic ship impact loads. *J. Offshore Mech. Arctic Engng* **114**, 146–153.

Thompson, J. M. T. 1983 Complex dynamics of compliant offshore structures. *Proc. R. Soc. Lond.* A **387**, 407–427.

Thompson, J. M. T., Bokaian, A. R. & Ghaffari, R. 1984 Subharmonic and chaotic motions of compliant offshore structures and articulated mooring towers. *J. Energy Resources Tech.* **106**, 191–198.

Tso, W. K. & Wong, C. M. 1989 Steady-state rocking response of rigid blocks. Part 1: analysis. *Earthquake engng Structural Dynamics* **18**, 89–106.

Tung, P. C. & Shaw, S. W. 1988 The dynamics of an impact print hammer. *J. Vib. Acoust. Stress Reliability Design* **110**, 193–200.

PHILOSOPHICAL TRANSACTIONS OF THE ROYAL SOCIETY A MATHEMATICAL, PHYSICAL & ENGINEERING SCIENCES